



Contents lists available at ScienceDirect

Bioorganic & Medicinal Chemistry Letters

journal homepage: www.elsevier.com/locate/bmcl

[¹¹C]Sorafenib: Radiosynthesis and preliminary PET study of brain uptake in P-gp/Bcrp knockout mice

Chiharu Asakawa^a, Masanao Ogawa^{a,b}, Katsushi Kumata^a, Masayuki Fujinaga^a, Koichi Kato^a, Tomoteru Yamasaki^a, Joji Yui^a, Kazunori Kawamura^a, Akiko Hatori^a, Toshimitsu Fukumura^a, Ming-Rong Zhang^{a,*}

^a Department of Molecular Probes, Molecular Imaging Center, National Institute of Radiological Sciences, 4-9-1 Anagawa, Inage-ku, Chiba 263-8555, Japan

^b SHI Accelerator Service Co. Ltd, 5-9-11 Kitashinagawa, Shinagawa-ku, Tokyo 141-8686, Japan

ARTICLE INFO

Article history:

Received 2 February 2011

Revised 28 February 2011

Accepted 1 March 2011

Available online 6 March 2011

Keywords:

[¹¹C]sorafenib

PET

P-gp

Bcrp, [¹¹C]phosgene

ABSTRACT

Sorafenib (Nexavar, BAY43-9006, **1**) is a second-generation, orally active multikinase inhibitor that is approved for the treatment of some cancers in patients. In this Letter, we developed [¹¹C]**1** as a novel positron emission tomography (PET) probe, and evaluated the influence of ABC transporters-mediated efflux on brain uptake using PET with [¹¹C]**1** in P-glycoprotein (P-gp)/breast cancer resistance protein (Bcrp) knockout mice versus wild-type mice. [¹¹C]**1** was synthesized by the reaction of hydrochloride of aniline **2** with [¹¹C]phosgene ([¹¹C]COCl₂) to give isocyanate [¹¹C]**6**, followed by reaction with another aniline **3**. Small-animal PET study with [¹¹C]**1** indicated that the radioactivity level (AUC_{0–60 min}, SUV × min) in the brains of P-gp/Bcrp knockout mice was about three times higher than in wild-type mice.

© 2011 Elsevier Ltd. All rights reserved.

Sorafenib (Nexavar, BAY43-9006, **1**; Scheme 1) is a second-generation, orally active inhibitor of Raf kinase and vascular endothelial growth factor receptor.^{1,2} Because this drug has shown marked clinical efficacy and safety in advanced renal cell and hepatocellular carcinoma,^{3,4} it has been approved for the treatment of these cancers in patients.⁵ Recently, a few case reports showed that **1** can achieve partial remission in renal cell carcinoma patients with brain metastases.^{6,7} Although brain metastases containing leaky blood vessels due to neovascularization, brain tumors are often protected from adequate chemotherapy because they are still mostly behind the intact blood–brain barrier (BBB).⁸

It has been demonstrated that ATP-binding cassette (ABC) transporters, such as P-glycoprotein (P-gp, Abcb1a/1b) and breast cancer resistance protein (Bcrp, Abcg2), have a negative influence on chemotherapy efficacy against tumor cells. These transporters are located on the apical membranes of epithelial and endothelial barriers, limiting the distribution of drugs to tissues such as the brain and testis and facilitating excretion of drugs from the liver, intestines and kidneys.⁸ Moreover, overexpression of these transporters in tumor cells can result in significant chemoresistance to drugs.⁹ There have been many reports that that P-gp can limit

the entrance and distribution of anticancer drugs to the brain and cancer cells.^{10,11}

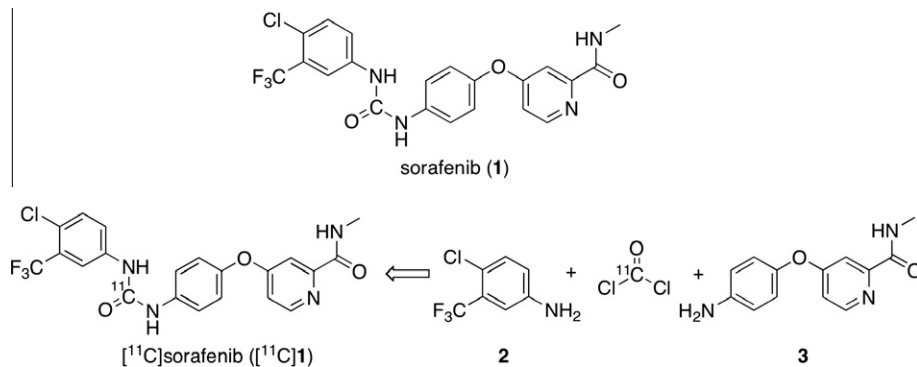
It has been reported that the penetration and accumulation of **1** in brain was limited by Bcrp and P-gp.^{12,13} To confirm the chemotherapeutic effect of **1** for brain metastases, it is important to evaluate and overcome the restriction of P-gp and Bcrp on the penetration of **1** into the brain. This motivated us to develop carbon-11-labeled **1** ([¹¹C]sorafenib, [¹¹C]**1**; Scheme 1) as a novel positron emission tomography (PET) probe and to visualize and qualify the influence of P-gp and Bcrp-mediated efflux on the brain uptake.

PET is a molecular and functional imaging technique with sensitivity, which permits repeated, non-invasive assessment and quantification of specific biological and pharmacological processes.¹⁴ It is playing an increasing role in both drug discovery and development by assessing their pharmacokinetics and pharmacodynamics. To evaluate functionality of P-gp and Bcrp at the BBB, we have developed [¹¹C]gefitinib¹⁵ and [¹¹C]topotecan,¹⁶ two anticancer drugs, which are substrates for Pgp and Bcrp. PET with both radioligands has shown that their brain uptake was significantly limited by P-gp and Bcrp.

In this Letter, we synthesized [¹¹C]**1** for the first time. Using small-animal PET with [¹¹C]**1**, we compared the brain uptake in P-gp/Bcrp knockout (Abcb1a/1b^{-/-}Abcg2^{-/-}) mice with that in wild-type mice and evaluated the effect of P-gp and Bcrp for the brain uptake of radioactivity.

* Corresponding author. Tel.: +81 43 382 3708; fax: +81 43 206 3261.

E-mail address: zhang@nirs.go.jp (M.-R. Zhang).



Scheme 1. Chemical structure of **1** and retrosynthesis of [^{11}C]**1**.

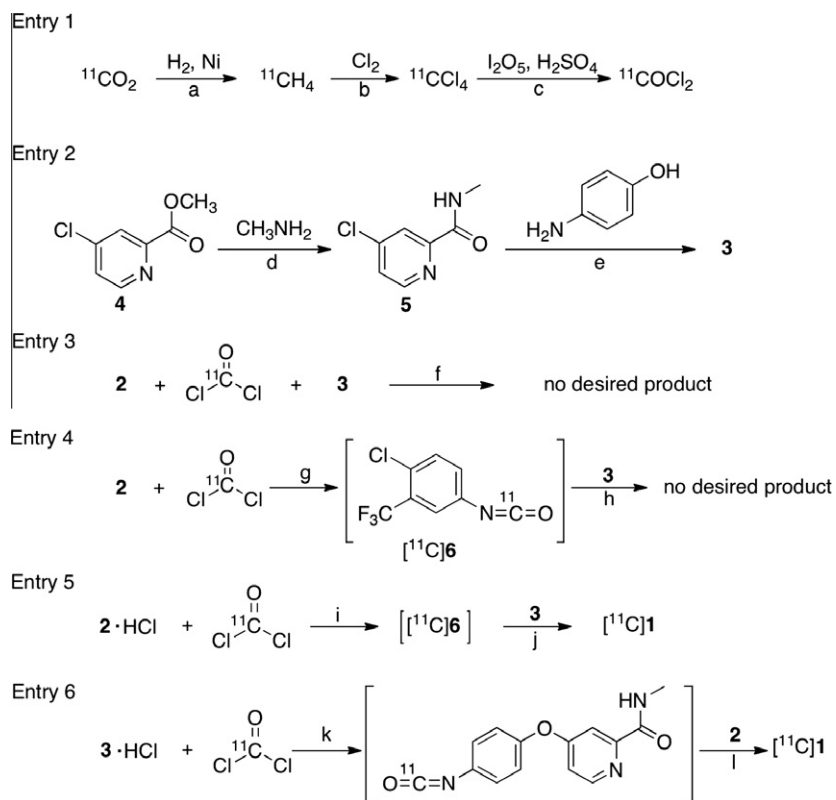
Regarding the chemical structure of **1** with an unsymmetrical urea moiety, we decided to label **1** using [^{11}C]phosgene ([^{11}C]COCl $_2$) as a labeling agent.¹⁷ This approach involves efficient construction of an unsymmetrical [^{11}C]urea site, which requires reliable preparation of [^{11}C]COCl $_2$, and uses two different anilines: 4-chloro-3-trifluoromethylaniline (**2**) and 4-(4-aminophenoxy)-*N*-methylpyridine-2-carboxamide (**3**), as shown in the retrosynthetic route (Scheme 1).

The preparation of [^{11}C]COCl $_2$ for the present radiosynthesis is routinely performed in our facility.^{18,19} As shown in entry 1 of Scheme 2, [^{11}C]COCl $_2$ was synthesized from cyclotron-produced [^{11}C]CO $_2$ via [^{11}C]CH $_4$ and [^{11}C]CCl $_4$ using a home-made automated production system.¹⁸ After irradiation, [^{11}C]CO $_2$ was recovered from the cyclotron target and cryogenically concentrated in a stainless steel tube. Release of [^{11}C]CO $_2$ from the tube, followed by passage of [^{11}C]CO $_2$ (50 mL/min) through a methanizer, gave

[^{11}C]CH $_4$,²⁰ which was mixed with chlorine gas and passed through a heated quartz tube at 560 °C to afford [^{11}C]CCl $_4$. [^{11}C]CCl $_4$ was continuously passed through a pretreated tube containing oxidizing agents, which is known as a Kitagawa gas detection tube for working-environmental CCl $_4$ concentration measurement,¹⁸ at room temperature to produce [^{11}C]COCl $_2$ at an average of 75% decay-corrected radiochemical yield, based on the starting [^{11}C]CO $_2$. This on-line production process took about 10 min from the end of bombardment.

As shown in entry 2 of Scheme 2, aniline **3** was prepared by reacting methyl 4-chloro-2-picolinate (**4**) with methylamine, followed by reaction with *p*-aminophenol in the presence of potassium *tert*-butoxide with a total chemical yield of 57% from **4**.²¹

Before automated synthesis of [^{11}C]**1** using our own equipment, we examined the reaction conditions for constructing the unsymmetrical [^{11}C]urea moiety, as shown in entries 3–6 of Scheme 2.



Scheme 2. Chemical synthesis and radiosynthesis. Reagents and conditions: (a) 400 °C, 2 min; (b) 560 °C, 2 min; (c) rt, 2 min, 70–80% from [^{11}C]CO $_2$; (d) CH $_3$ OH, 50 °C, 5 h, 59%; (e) *t*-BuOK, DMF, 25 °C, 1 h, 97%. (f) THF, –15 °C, 1 min; (g) THF, –15 °C, 1 min; (h) THF, 60 °C, 3 min; (i) THF, –15 °C, 1 min; (j) THF, 60 °C, 3 min, 91% (incorporation of total radioactivity in the final reaction mixture); (k) THF, –15 °C, 1 min; (l) THF, 60 °C, 3 min, 40% (incorporation of total radioactivity in the final reaction mixture).

The forming efficiency of [^{11}C]**1** (decay-corrected) in the reaction mixture was analyzed by HPLC.

Firstly, [^{11}C]COCl₂ gas was bubbled into a THF solution containing a mixture of **2** (0.5 mg, 2.56 μmol) and **3** (0.62 mg, 2.56 μmol) at $-15\text{ }^\circ\text{C}$ for 1 min (entry 3). However, no radioactive peak corresponding to [^{11}C]**1** was detected in the reaction mixture, except for two symmetrical [^{11}C]ureas of **2** and **3**, respectively.

The next approach was to apply isocyanate [^{11}C]**6** as a radioactive intermediate, which was formed by the reaction of [^{11}C]COCl₂ with **2** in THF at $-15\text{ }^\circ\text{C}$ during the trapping process for 1 min (entry 4). Without purification of [^{11}C]**6**, another aniline **3** was immediately added to this reaction mixture. However, no [^{11}C]**1** was

found in the final reaction mixture except for the symmetrical [^{11}C]urea of **2**. Increasing the amount of **3** from 1- to 100-fold relative to **2** did not achieve the formation of [^{11}C]**1**, although this treatment has been used to synthesize two PET probes containing an unsymmetrical [^{11}C]urea moiety, as reported previously.^{22,23} Changing the reaction solvent from THF to dioxane, CH₃CN, DMF or CH₂Cl₂ did not accelerate the synthesis of [^{11}C]**1** and even decreased the trapping efficiency of [^{11}C]COCl₂ in some solvents.

We assumed that [^{11}C]**6** was difficult to retain in the mixture containing **2** within the trapping of [^{11}C]COCl₂. Because the mass of **2** was excessive relative to that of [^{11}C]COCl₂, the formed [^{11}C]**6** further reacted with **2** to produce the symmetrical [^{11}C]urea. To decrease the nucleophilicity of **2**, we used hydrochloride of **2** (**2**·HCl) in place of the free **2** (entry 5). As expected, the nucleophilicity of **2**·HCl was enough to react with [^{11}C]COCl₂ perfectly to give [^{11}C]**6** even at $-15\text{ }^\circ\text{C}$. After subsequent treatment of [^{11}C]**6** with **3**, the desired [^{11}C]**1** was produced with 91% incorporation of the total radioactivity in the reaction mixture. On the other hand, the reaction of hydrochloride of **3** (**3**·HCl) with [^{11}C]COCl₂, followed by subsequent reaction with **2**, also afforded [^{11}C]**1** with 40% incorporation of the total radioactivity in the reaction mixture (entry 6).

According to the reaction conditions determined here, we carried out entirely automated synthesis of [^{11}C]**1**. [^{11}C]COCl₂ gas (50 mL/min) was bubbled into a solution of **2**·HCl (0.25 mg, 1.08 μmol in 300 μL THF) at $-15\text{ }^\circ\text{C}$ for 1 min, followed by reaction of **3** (0.52 mg, 2.16 μmol in 300 μL THF) at $60\text{ }^\circ\text{C}$ for 3 min. After the two-step reactions, THF was removed. The reaction mixture was diluted with HPLC solvent and applied onto a reversed-phase HPLC system. Figure 1A shows a representative HPLC chromatogram for separation, which shows that [^{11}C]**1** was produced as the main radioactive peak in the reaction mixture. Starting at 15.5–22.2 GBq of [^{11}C]CO₂, 1.2–2.5 GBq of [^{11}C]**1** was obtained at the end of synthesis ($n = 8$). The total synthesis time was averaged as 40 min from the end of bombardment.

The identity of [^{11}C]**1** was confirmed by co-injection with non-radioactive **1** on analytic HPLC. In the final product solutions, the radiochemical purity of [^{11}C]**1** was higher than 99% (Fig. 1B) and specific activity was 20–56 GBq/ μmol ($n = 8$). No significant UV peaks corresponding to **2**, **3** and other chemical impurities were observed on HPLC charts of the finally-formulated product. Moreover, the radiochemical purity of [^{11}C]**1** remained >98% after 120 min at

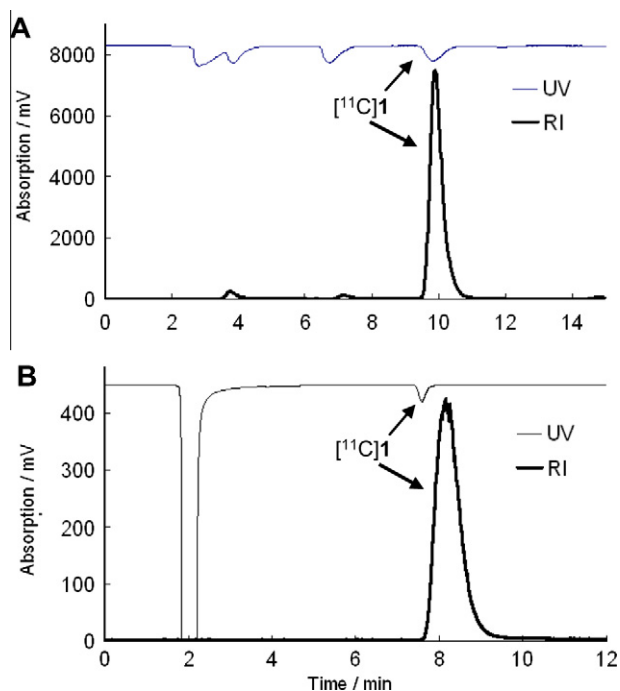


Figure 1. Chromatograms from the HPLC separation (A) and analysis (B) used in the radiosynthesis of [^{11}C]**1**.

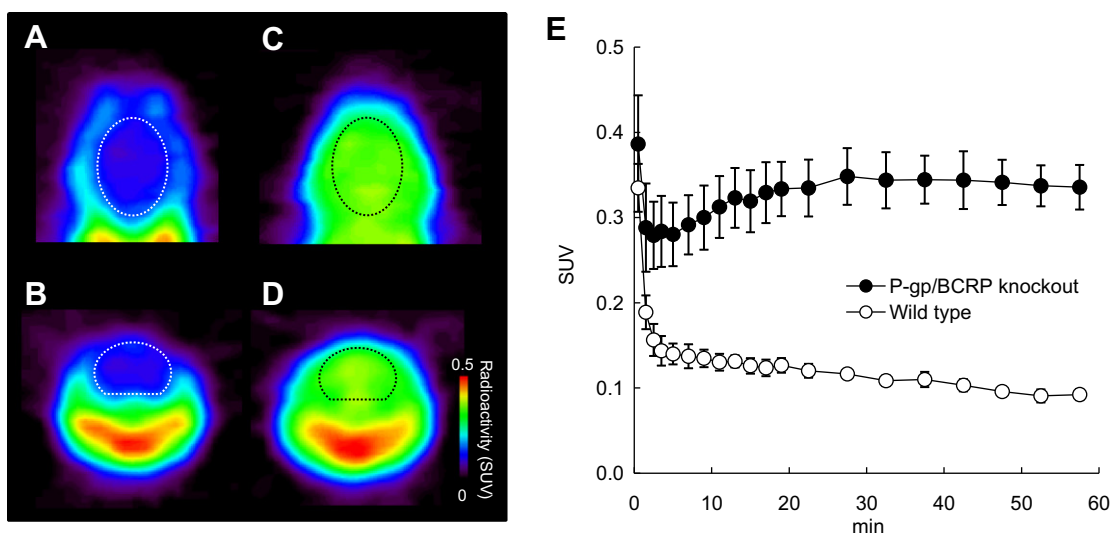


Figure 2. PET imaging of the brains in wild-type and P-gp/Bcrp knockout mice. (A) and (B) are images of wild-type mouse, and (C) and (D) are images of P-gp/Bcrp knockout mouse. (A) and (C) are coronal images, and (B) and (D) are horizontal images. (E) shows the time-activity curves in the brains of wild-type- and P-gp/Bcrp knockout mice. Data are the means \pm SD ($n = 3$ for each group).

room temperature, and this probe was radiochemically stable for the time of one PET scan. These analytical results were in compliance with our in-house quality control/assurance specifications.

To determine brain radioactivity (expressed as standardized uptake value: SUV), we performed PET with [¹¹C]**1** on wild-type and Pgp/Bcrp knockout mice using a small-animal PET scanner.²⁴ Figure 2A and B shows representative brain PET images of coronal and horizontal views in a wild-type mouse. The brain uptake of radioactivity in wild-type mice was quite low. Figure 2C and D shows representative brain PET images in P-gp/Bcrp knockout mice, in which radioactivity accumulation was seen. The brain uptake in the knockout mice was higher than that in wild-type mice. Figure 2E shows the time-activity curves in the brains of two groups. The radioactivity levels, represented as values of area under the time-activity curves (AUC_{0–60 min}, SUV × min), in the brain between 0 and 60 min after injection of [¹¹C]**1** were 18.83 ± 1.80 (n = 3) for P-gp/Bcrp knockout mice and 6.72 ± 0.40 (n = 3) for wild-type mice, respectively. The difference in the AUC_{0–60 min} values of brains was statistically significant between the two groups (P < 0.05, Student's paired t-test). As a control, there was no significant difference in the AUC_{0–60 min} values of the cardiac blood pool between the two groups of mice (data not shown).

These results indicated that the brain uptake related to [¹¹C]**1** was limited by P-gp and Bcrp at the BBB. The brain uptake of radioactivity in P-gp/Bcrp knockout mice was increased by deficiency of P-gp and Bcrp functions at the BBB. This Letter may enable evaluation of the bioavailability of **1** in combination chemotherapy against brain tumors. PET study with [¹¹C]**1** may provide useful information for the treatment of renal cell carcinoma patients with brain metastases, because a dual Bcrp and P-gp inhibitor, such as elacridar,^{25,26} may improve brain permeability and thereby the therapeutic efficacy of **1**. Moreover, PET with [¹¹C]**1** may be used to evaluate anticancer therapeutic effects of other molecular target drugs, such as gefitinib^{15,27} and imatinib,²⁸ which are also substrates for P-gp and Bcrp.

In conclusion, [¹¹C]**1** was successfully labeled with carbon-11 at its urea site using [¹¹C]COCl₂ as a labeling agent, via the intermediate preparation of isocyanate [¹¹C]**6**. The preliminary results indicated that [¹¹C]**1** is a promising PET probe for evaluating the therapeutic efficiency of **1** for brain tumors. Studies on the effect of P-gp or/and Bcrp modulators on the penetration of **1** into brain tumors and imaging of modeled animals bearing tumor are in progress.

Acknowledgments

We are grateful to Mrs. Y. Yoshida and N. Nobuki (SHI Accelerator Service Co. Ltd) for technical support with radiosynthesis, and to Mr. H. Wakizaka (National Institute of Radiological Sciences) for assistance with PET scans. We also thank the staff of the National Institute of Radiological Sciences for support with the cyclotron operation and radionuclide production.

References and notes

- Lyons, J. F.; Wilhelm, S.; Hibner, B.; Bollag, G. *Endocr. Relat. Cancer* **2001**, *8*, 219.
- Wilhelm, S. M.; Carter, C.; Tang, L.; Wilkie, D.; McNabola, A.; Rong, H.; Chen, C.; Zhang, X.; Vincent, P.; McHugh, M.; Cao, Y.; Shujath, J.; Gawlak, S.; Eveleigh, D.; Rowley, B.; Liu, L.; Adnane, L.; Lynch, M.; Auclair, D.; Taylor, L.; Gedrich, R.; Voznesensky, A.; Riedl, B.; Post, L. E.; Bollag, G.; Trail, P. A. *Cancer Res.* **2004**, *64*, 7099.
- Kane, R. C.; Farrell, A. T.; Saber, H.; Tang, S.; Williams, G.; Jee, J. M.; Liang, C.; Booth, B.; Chidambaram, N.; Morse, D.; Sridhara, R.; Garvey, P.; Justice, R.; Pazdur, R. *Clin. Cancer Res.* **2006**, *12*, 7271.
- Escudier, B.; Eisen, T.; Stadler, W. M.; Szczylik, C.; Oudard, S.; Siebels, M.; Negrier, S.; Chevreau, C.; Solska, E.; Desai, A. A.; Rolland, F.; Demkow, T.; Hutson, T. E.; Gore, M.; Freeman, S.; Schwartz, B.; Shan, M.; Simantov, R.; Bukowski, R. M. TARGET Study Group. *N. Eng. J. Med.* **2007**, *356*, 125.
- Wilhelm, S. M.; Adnane, L.; Newell, P.; Villanueva, A.; Liovet, J. M.; Lynch, M. *Mol. Cancer Ther.* **2008**, *7*, 3129.
- Ranze, O.; Hofmann, E.; Distelrath, A.; Hoeffkes, H. G. *Onkologie* **2007**, *30*, 450.
- Valcamonica, F.; Ferrari, V.; Amoroso, V.; Rangoni, G.; Simoncini, E.; Marpicati, P.; Vassalli, L.; Grisanti, S.; Marini, G. *J. Neurooncol.* **2009**, *91*, 47.
- de Vries, N. A.; Beijnen, J. H.; Boogerd, W.; van Tellingen, O. *Expert Rev. Neurother.* **2006**, *6*, 1199.
- Gottesman, M. M.; Pastan, I. *Annu. Rev. Biochem.* **1993**, *62*, 385.
- Schinkel, A. H.; Wagenaar, E.; van Deemter, L.; Mol, C. A.; Borst, P. *J. Clin. Invest.* **1995**, *96*, 1698.
- Dai, H.; Marbach, P.; Lemaire, M.; Hayes, M.; Elmquist, W. F. *J. Pharmacol. Exp. Ther.* **2003**, *304*, 1085.
- Gnoth, M. J.; Sandmann, S.; Engel, K.; Radtke, M. *Drug Metab. Dispos.* **2010**, *38*, 1341.
- Lagas, J. S.; van Waterschoot, R. A.; Sparidans, R. W.; Wagenaar, E.; Beijnen, J. H.; Schinkel, A. H. *Mol. Cancer Ther.* **2010**, *9*, 319.
- Fowler, J. S.; Volkow, N. D.; Wang, G.-J.; Ding, Y.-S.; Dewey, S. L. *J. Nucl. Med.* **1999**, *40*, 1154.
- Kawamura, K.; Yamasaki, T.; Yui, J.; Hatori, A.; Konno, F.; Kumata, K.; Konno, F.; Irie, T.; Fukumura, T.; Suzuki, K.; Kanno, I.; Zhang, M.-R. *Nucl. Med. Biol.* **2009**, *36*, 239.
- Yamasaki, T.; Fujinaga, M.; Kumata, K.; Kawamura, K.; Yui, J.; Hatori, A.; Zhang, M.-R. *Nucl. Med. Biol.* **2011**, *38*. doi:10.1016/j.nucmedbio.2010.12.012.
- Roeda, D.; Dollé, F. *Curr. Top. Med. Chem.* **2010**, *10*, 1680.
- Ogawa, M.; Takada, Y.; Suzuki, H.; Nemoto, K.; Fukumura, T. *Nucl. Med. Biol.* **2010**, *37*, 73.
- Takada, Y.; Ogawa, M.; Suzuki, H.; Nemoto, K.; Fukumura, T. *Appl. Radiat. Isot.* **2010**, *68*, 1715.
- Link, J. M.; Krohn, A. J. *Labelled Compd. Radiopharm.* **1997**, *40*, 306.
- Compound **3** [4-(4-aminophenoxy)-N-methylpyridine-2-carboxamide]: mp: 105–106 °C. ¹H NMR (300 MHz, CDCl₃) δ: 2.78 (3H, d, J = 4.77 Hz), 5.17 (2H, dd, J = 8.80, 1.83 Hz), 6.64 (2H, dd, J = 8.80, 1.83 Hz), 6.86 (1H, dd, J = 8.80, 1.83 Hz), 7.05–7.08 (1H, m), 7.34 (1H, d, J = 2.20 Hz), 8.45 (1H, d, J = 5.50 Hz), 8.73 (1H, br). FAB-MS calcd for C₁₃H₁₃N₃O₂: 243.27; found: 244 (M+H⁺).
- Conway, T.; Diksic, M. *J. Nucl. Med.* **1988**, *29*, 1957.
- Dollé, F.; Martarello, L.; Bramoullé, Y.; Bottlaender, M.; Gee, A. D. *J. Labelled Compd. Radiopharm.* **2005**, *48*, 501.
- A mouse was secured in a custom-designed chamber and placed in a small-animal PET scanner (Inveon; Siemens Medical Solutions, Knoxville, TN). Body temperature was maintained with a 40 °C water circulation system (TPump TP401, Gaymar Industries, Orchard Park, NY). The mouse was kept under anesthesia with 1.5% isoflurane during the scan. To inject [¹¹C]**1**, a 29-gauge needle with 12–15 cm of PE 10 tubing was placed into a tail vein of the mouse. A dynamic emission scan in 3D list-mode was performed for 60 min (1 min × 4 scans, 2 min × 8 scans, 5 min × 8 scans). A bolus of 11–16 MBq of [¹¹C]**1** in 100 μL saline was injected through the tail vein catheter. Wild-type (male; 17–18 w.o.; 30–32 g; n = 3) and P-gp/Bcrp knockout (Abcb1a/1b^{-/-}Abcg2^{-/-}; male; 17–18 w.o.; 31–33 g; n = 3) mice (FVB; Taconic Farm; Hudson, NY) were used in the PET experiments. Region-of-interest (ROI) analysis and image reconstruction were performed using the software ASIPro (Siemens Medical Solutions). Visual analysis was performed by individuals experienced in PET interpretation using coronal, horizontal, and sagittal reconstructions. ROIs were manually placed across image planes for time-activity curves. Radioactivity was decay-corrected to the injection time and expressed as a standardized uptake value (SUV), normalized for injected radioactivity and body weight: SUV = (radioactivity per milliliter tissue/injected radioactivity) × body weight in grams. The area under the time-activity curve of the ROIs in the brain (AUC_{0–60 min}, SUV × min) was calculated starting from 0 to 60 min.
- Yamasaki, T.; Kawamura, K.; Hatori, A.; Yui, J.; Yanamoto, K.; Yoshida, Y.; Ogawa, M.; Nengaki, N.; Fukumura, T.; Zhang, M.-R. *Nucl. Med. Commun.* **2010**, *31*, 985.
- Kawamura, K.; Yamazaki, T.; Konno, F.; Yui, J.; Hatori, A.; Yanamoto, K.; Wakizaka, H.; Fukumura, T.; Zhang, M.-R. *Mol. Imaging Biol.* **2011**, *13*, 152.
- Zhang, M.-R.; Kumata, K.; Hatori, A.; Takai, N.; Toyohara, J.; Yanamoto, K.; Yamasaki, T.; Yui, J.; Kawamura, K.; Koike, S.; Ando, K.; Suzuki, K. *Mol. Imaging Biol.* **2010**, *12*, 181.
- Lagas, J. S.; Waterschoot, R. A.; Tilburg, V. A.; Hillebrand, M. J.; Lankheet, N.; Rosing, H.; Beijnen, J. H.; Schinkel, A. H. *Clin. Cancer Res.* **2009**, *15*, 2344.